ARTHRITIS & RHEUMATOLOGY
Vol. 66, No. 8, August 2014, pp 2071–2078
DOI 10.1002/art.38642

Optoacoustic Imaging and Staging of Inflammation in a Murine Model of Arthritis

N. Beziere,[1] C. von Schacky,[2] Y. Kosanke,[2] M. Kimm,[2] A. Nunes,[1] K. Licha,[3] M. Aichler,[4] A. Walch,[4] E. J. Rummeny,[2] V. Ntziachristos,[1] and R. Meier[2]

Objective. **Rheumatoid arthritis (RA) is one of the most frequent inflammatory diseases, causing pain and disability in the affected joints. Early diagnosis is essential for the efficiency of symptom-targeting treatments, but its diagnosis requires careful clinical, serologic, and imaging examinations, such as magnetic resonance imaging (MRI), which is both expensive and time consuming. In an effort to provide the biomedical community with a more accessible way to assess the advancement of arthritis, this study sought to investigate the use of multispectral optoacoustic tomography (MSOT) in a murine arthritis model, to visualize the extent of inflammation in vivo through an L-selectin/P-selectin–targeting contrast agent.**

Methods. **Mice with collagen-induced arthritis were studied as a model of RA. MSOT was performed using an L-selectin/P-selectin–targeting contrast agent, polyanionic dendritic polyglycerol sulfate (dPGS) labeled with a near-infrared (NIR) fluorophore, to increase the contrast of the arthritic joint. The signal intensity ratios between healthy legs and arthritic legs were calculated. Findings on contrast-enhanced MRI, clinical observations, the lymphocyte:granulocyte ratio, and histologic findings served as referents for comparison.**

Results. **MSOT using an inflammation-targeting contrast agent, dPGS-NIR, allowed for accurate diagnosis of inflammation in the mouse joints. In addition, use of this technique resulted in significant differentiation of the inflamed joints from the healthy joints ($P = 0.023$). The observed advancement of arthritis on the MSOT images was confirmed by clinical observation, blood analysis, contrast-enhanced MRI, and ex vivo histologic examinations.**

Conclusion. **This study demonstrates that the combination of an inflammation-targeting contrast agent and optoacoustic tomographic imaging presents a promising means for the diagnosis of RA and the staging of arthritis-related inflammation.**

Rheumatoid arthritis (RA) is a chronic autoimmune inflammatory disease that is characterized by inflammation of the synovium, resulting in the destruction of cartilage and bone in the joints. Improvement of the clinical outcome in RA relies on early and aggressive treatment, enabled by early diagnosis through a combination of clinical, laboratory, and imaging data. In the field of imaging, specific and sensitive tools tailored toward the detection of inflammation are needed to overcome the limitations of classic imaging techniques (1). Even though radiographic imaging of the joints is used for clinical evaluation, radiographs show advanced bone degradation only years after the start of inflammation (2). Ultrasound and magnetic resonance imaging (MRI) have been found to be an improvement over classic radiography (3–5), but these techniques are lim-

Drs. Beziere, Nunes, and Ntziachristos' work was supported by the European Union Seventh Framework Programme (Research and Technology Development grant 2007-2013 FMT-XCT) and the Cluster of Excellence project Nanosystem Initiative Munich. Mr. von Schacky and Drs. Kosanke, Kimm, Rummeny, and Meier's work was supported by the BMBF (Cluster of Excellence project M4 Individualized Medicine). Drs. Aichler and Walch's work was supported by the DFG (SFB grant 824, Project Z2).

[1]N. Beziere, PhD, A. Nunes, PhD, V. Ntziachristos, PhD: Technische Universität München, Munich, Germany, and Helmholtz Zentrum München, Neuherberg, Germany; [2]C. von Schacky, MS, Y. Kosanke, PhD, M. Kimm, PhD, E. J. Rummeny, MD, PhD, R. Meier, MD, PhD: Technische Universität München, Munich, Germany; [3]K. Licha, PhD: Mivenion GmbH, Berlin, Germany; [4]M. Aichler, PhD, A. Walch, PhD: Helmholtz Zentrum München, Neuherberg, Germany.

Mivenion GmbH holds patent WO2011095311 for dPGS and its use as a targeting moiety for near-infrared imaging. Dr. Licha is the inventor of this technique. Dr. Ntziachristos owns stock or stock options in Ithera Medical GmbH.

Address correspondence to Nicolas Beziere, PhD, Institute for Biological and Medical Imaging, Technische Universität München, Ismaningerstrasse 22, D-81675 Munich, Germany. E-mail: Nicolas.beziere@tum.de.

Submitted for publication September 27, 2013; accepted in revised form March 20, 2014.

ited by high interoperator variability and high cost, respectively.

Overall, a broad panel of techniques is available to the clinician today, each of which gives access to high-quality anatomic data. Through the use of contrast agents, these techniques can provide insight into certain pathophysiologic events, namely permeability of the synovium. However, no technology available widely in the clinic for the diagnosis of arthritis provides functional molecular imaging data for accurate evaluation of the advancement of arthritis and the state of its activity. This can be enabled with the use of optical methods in which carefully chosen and tailored contrast agents are employed.

An interesting approach is the use of fluorescent reporters, which are small organic molecules that have the double benefit of 1) being extremely stable when compared to positron emission tomography contrast agents, and 2) allowing various functional characterizations through chemical branching. It is already possible, with the use of US Food and Drug Administration (FDA)–approved contrast agents such as indocyanine green (ICG) and epifluorescence equipment (6–9), to observe hyperperfusion and retention in the inflamed joint. However, with the correct targeting moiety attached, fluorescence-based observation of the inflamed sites becomes possible (10,11), with no ionizing radiation or expensive equipment required.

Such a strategy has recently been pushed one step forward by the development of an L-selectin/P-selectin–targeting contrast agent, namely a polyglycerol sulfate polymer, polyanionic dendritic polyglycerol sulfate (dPGS), as a therapeutic approach for attenuating inflammation, since these glycoproteins are implicated in the leukocyte recruitment process (12). In an RA model in which protein labeling with fluorescent probes was utilized, it was shown that the whole construct accumulates in the region of the inflamed joint in amounts directly related to the stage of the disease, constituting an interesting theranostic approach (13). However, results in vivo failed to reveal volumetric changes and only showed epifluorescence of accumulation of the contrast agent in the joints, with a marked difference between the inflamed site and the healthy site. Overall, these results seem promising but are limited in their clinical translation by the technology used, notably the shallow penetration depth of classic fluorescence imaging, even in the near-infrared (NIR) window of the electromagnetic spectrum.

One possible way to circumvent this limitation is to move away from purely optical techniques for imaging and exploit the optoacoustic effect, which capitalizes on the emission of ultrasound waves that are generated by thermal expansion of samples after absorption of pulsed-light energy. Since the scattering of ultrasound waves is order of magnitudes smaller than optical scattering, the penetration depth and resolution attainable using optoacoustic imaging in which optical contrast is still retained is unmatched by other optical imaging methods (14). A recent evolution of this technique, called multispectral optoacoustic tomography (MSOT) (15), shows promising performance in mapping and identifying different photoabsorbers in real time in a living animal, using an unmixing method for spectral identification. MSOT enables molecular and functional imaging of the joints (16) in conjunction with simultaneous gathering of anatomic data, an approach that is notably facilitated by the specific absorbance spectra of hemoglobin, oxygenated hemoglobin, and fat (17,18). Use of MSOT has led to new insights into the behavior and biodistribution of photoabsorbers, such as the FDA-approved fluorophore ICG (19), or nanoparticles, such as gold nanostructures (20).

Recently, dPGS-based fluorophores have been imaged by MSOT (21) as a tool to visualize the extent of a heart infarct caused by artery ligation in a mouse model. Optoacoustic imaging has also been utilized recently to identify and monitor the treatment of RA in rat ankles (22,23), an approach that involved red and infrared light, relied solely on angiogenesis as a nonspecific disease marker, and provided a single transverse slice of the potentially affected joints. Very recently, in a study in which tumor necrosis factor α–targeting strategies were used, gold nanoparticles were investigated for proof of concept that the contrast for optoacoustic imaging of arthritis would be increased (24). Although that study provided interesting results, the approach chosen did not allow for staging or accurate mapping of the inflamed area. Additionally, gold nanorods are not easily excreted, which presents a major hindrance for possible clinical translation. Comparatively, the purpose of the present study was to evaluate MSOT using a fully organic, inflammation-targeting contrast agent as a tool for the diagnosis of RA in a preclinical model, with clinical observation and MRI used as referents for comparison. We aimed to build on this newly developed tomographic and multispectral approach in order to overcome the limitations previously observed and, ultimately, to accurately stage and map the spread of inflammation in RA.

MATERIALS AND METHODS

Animal model. All animal experiments were performed with approval from the government of Upper Bavaria (reference no. 55.2-1-54-2532-179-11). In total, 14 male DBA/1 mice ages 7–8 weeks (Janvier Labs, France) were randomly categorized into 1 of 2 groups. One group comprised 12 mice subjected to collagen induction of arthritis, and the other group comprised 2 untreated control mice. The murine model of collagen-induced arthritis (CIA) is widely used because of its similarity to human RA (25).

For the induction of arthritis, Freund's complete adjuvant, which consists of mineral oil and heat-killed *Mycobacterium tuberculosis* at a concentration of 1 mg/ml, and a phosphate buffered saline (PBS) solution containing bovine type II collagen at a concentration of 1 mg/ml were mixed together in a ratio of 1:1. Twenty microliters of this compound was injected below the left knee of each mouse, as previously described in a study by Kamala et al (26). After 3 weeks, the injected animals received a booster injection in the same limb. Within ~25–30 days thereafter, the mice were expected to develop severe arthritis in the injected leg. Only mice that developed arthritis, as determined by clinical examination, were used for the imaging experiments.

Clinical examination. All animals were examined daily for their general state of health and, specifically, for arthritis-associated symptoms such as swelling, redness, and lameness in the legs. Blood samples were obtained once per week from the facial vein of each mouse to analyze the ratio of lymphocytes to granulocytes. This ratio is typically low in the acute phase of inflammation, whereas chronic inflammation typically manifests as a high ratio of lymphocytes to granulocytes.

MSOT contrast agent. The contrast agent that was used in MSOT is based on a dPGS that is able to bind to P- and L-selectins, thereby reducing the extravasation of leukocytes (12,13) (a complete description of the synthesis of the dPGS-NIR contrast agent is available from the corresponding author upon request). The two absorbance peaks in the near-infrared for dPGS-NIR are located at 710 nm and 795 nm, and the maximum fluorescence emission is 810 nm with a quantum yield of roughly 1%, thus providing an efficient agent for MSOT imaging.

For ex vivo histology studies, the contrast agent comprised dPGS with a fluorescent indocarbocyanine conjugate (ICC), a structural analog of dPGS-NIR that uses a fluorophore with absorption in the visible range (propargyl, with absorption of 550 nm and emission peak of 570 nm; Mivenion). Use of this dPGS-ICC contrast agent enabled detection of changes in the joints with standard fluorescence microscopes at a higher sensitivity than could be achieved using NIR fluorescence. For the optoacoustic imaging experiments and histopathology, 7.5 mg/kg of the corresponding contrast agent was injected intravenously.

Imaging. MSOT and MRI experiments were performed in the animals at a mean 32 days (±SD 2 days) after the induction of arthritis.

MSOT system for whole-body imaging. All MSOT measurements were performed in a real-time optoacoustic imaging system, as previously described (17) (a full description is available from the corresponding author upon request). During the procedure, all animals were kept under anesthesia using a mixture of 1.8% isoflurane in air.

Imaging was performed before, immediately after, and 150 minutes after injection of the contrast agent for each animal, because a time window of 2 hours 30 minutes presents the best contrast-to-noise ratio, as has been established in previous studies (21) and as confirmed experimentally using various time points up to 240 minutes. Each animal was positioned with the legs stretched in a similar manner on the left and right side, in order to be able to compare the results easily. Imaging of the animals was performed from the toes to the hips using 0.5-mm steps, which allowed us to image the whole region of possible inflammation. Data acquisition was performed using 30 averages per illumination wavelength, with the wavelengths chosen as follows: 700 nm, 730 nm, 760 nm, 800 nm, 830 nm, and 860 nm. These illumination wavelengths were chosen in order to maximize the efficiency of the processing methods, as they were determined on the basis of the spectral characteristics of the main photoabsorbers, namely oxyhemoglobin, deoxyhemoglobin, and dPGS-NIR (details available from the corresponding author upon request), while the acquisition time was kept to a minimum. This resulted in an acquisition time of ~20 minutes.

MRI. MRI scans were performed using a 1.5T clinical MR system (Achieva; Philips Medical Systems). During the MRI scan, the mice were fixated with their legs moderately and symmetrically stretched while being kept under anesthesia using a gaseous infusion of isoflurane at 1.5–2% in air. A surface coil was positioned around both knees. A standard MRI protocol was utilized to assess arthritis in both knees of each mouse (details on the MRI protocol are available from the corresponding author upon request). The overall acquisition time was ~40 minutes.

Imaging analysis. *MRI.* The MRI findings were evaluated by a radiologist (RM) who is experienced in imaging of arthritis. Synovitis was scored on a scale of 0–3 in each joint, with a score of 0 representing no synovitis and scores of 1–3 representing mild, moderate, and severe arthritis, respectively. Synovitis was defined as an abnormal increase in signal intensity in the area of the synovium after gadolinium injection, and an expanded synovial membrane.

MSOT system for whole-body imaging. For processing of the MSOT data, we used a model-based reconstruction process, as described previously (27,28), followed by spectral unmixing based on spectral fitting by the least-squares method, using the absorbance spectra of hemoglobin, oxygenated hemoglobin, and the contrast agent. Because the absorbance of bone in the selected range of wavelengths was negligible in comparison, its contribution was omitted from the analysis.

For further data processing, MatLab software with a custom-made script was used. In the transverse image containing the articulations, 2 distinct regions of interest were chosen using the image acquired at 800-nm illumination, encompassing the whole articulation for the left and right side. The overall maximum value of the dPGS-NIR signal in the regions of interest was then extracted and used to establish the threshold for the signal at 20% of the maximum value, to remove excess noise. As a last step, summing the values for the 25% of pixels showing the most intensity in each region of interest provided an overall value of the probe accumulation on each side. By determining the ratio of the articulation in the

arthritic joint to that in the healthy joint, a score of overall inflammation was obtained. Absolute values of this difference were used to ensure the accuracy of the method. Furthermore, the volume of blood circulating in the vicinity of the joints was estimated by first determining a threshold for normal blood circulation, and subsequently counting the pixels for the hemoglobin and oxygenated hemoglobin signals above the threshold.

The value resulting from the MSOT comparison of the accumulation of the probe in the knees was matched to the stage of CIA in the animals. The different stages (healthy, low inflammation, and high inflammation) were defined on the basis of a mixture of clinical and MRI findings.

Histopathology. After the imaging experiments, mice were killed by cervical dislocation, and thereafter stored at −80°C until used in validation studies. For the histologic analysis of arthritis, specimens injected with the dPGS-ICC probe were fixed in formalin and decalcified in Osteosoft (Merck), according to the manufacturer's instructions. Sections of 4-μm thickness were cut and stained with hematoxylin and eosin. Fluorescence images of probe-injected samples were captured using an Axio Imager Z1 upright microscope system (Carl Zeiss). ICC-based contrast agents were detected with a 43 HE DsRed filter set (Carl Zeiss). Nuclei were identified with Hoechst 33342 dye (filter set 49 DAPI; Carl Zeiss).

The histologic grading of inflammation was determined in a blinded manner, with grades ranging from 0 to 3 for each limb as follows: grade 0 = no changes, grade 1 = few focal infiltrates, grade 2 = extensive focal infiltrates, and grade 3 = extensive infiltrates invading the capsule.

RESULTS

Clinical examination findings. Overall, 6 of the 12 experimental mice injected with collagen developed severe arthritis, with marked clinical manifestations such as redness, swelling, and lameness in the leg joints as well as an elevated lymphocyte:granulocyte ratio 30 days after the induction of arthritis (further data are available from the corresponding author upon request). Clinical manifestations of RA were not observed in a healthy control mouse with a normal lymphocyte:granulocyte ratio of ~3:1.

Results of in vivo imaging. MSOT at 2 hours 30 minutes after injection of the L-selectin/P-selectin–targeting contrast agent dPGS-NIR into the mouse limbs provided optimal contrast between the healthy legs and arthritic legs, as compared to that at various time points up to 240 minutes (results not shown). The processed MSOT images revealed a clear difference between the right (healthy) and left (arthritic) side of animals that had received a collagen injection and had developed symptoms of inflammation. Depending on the extent of advancement of the arthritis and its clinical characteristics, a significant increase in the MSOT signal of >35% could be seen in the arthritic joints of all mice in which synovitis was evident on MRI, whereas only one healthy mouse showed aberrant accumulation of the probe in only one limb (P = 0.023 for the average of measured signal in inflamed joints versus the average of measured signal in normal joints).

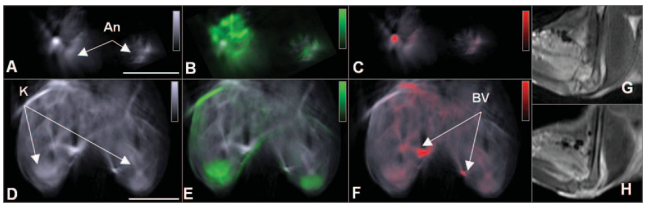

Figure 1. Multispectral optoacoustic tomography (MSOT) imaging of the ankles (**An**) and knees (**K**) of a representative mouse at an advanced stage of arthritis, using near-infrared (NIR) imaging with polyanionic dendritic polyglycerol sulfate (dPGS) contrast agent. **A–F,** MSOT images of the left and right ankles (**A**) and knees (**D**) were acquired at an illumination wavelength of 860 nm for anatomic contrast. MSOT signals for dPGS-NIR accumulation and oxygenated hemoglobin in the ankles (**B** and **C**) and in the knees (**E** and **F**) are shown as fluorescence overlays on the anatomic images. Part of the bladder is also visible. Bars = 5 mm. **G** and **H,** Sagittal T1-weighted magnetic resonance images were obtained from the left knee joint of the same mouse before (**G**) and after (**H**) gadolinium injection. **BV** = blood vessel.

Figure 1 shows an example of an animal at an advanced stage of arthritis as detected on clinical examination, with evident swelling, redness, and rigidity of the limb. In MSOT images using a single illumination wavelength of 860 nm, the left joint appeared bigger than the right joint (Figures 1A and D). After multispectral unmixing, the signal identified, i.e., the accumulation of dPGS-NIR, appeared to occupy more pixels and also to be more intense in the left joint (Figures 1B and E).

Since a purely visual observation is insufficient to diagnose arthritis, to stage the inflamed area, and to potentially monitor treatment accurately, we developed a quantitative method for comparison of the left (arthritic) and right (healthy) joints in our animal model. In the representative animal shown in Figure 1, this translates into a signal increase of ~72% between the left and right joints, with the signal from the healthy side presenting a dPGS-NIR signal value of 83 arbitrary units (AU), compared to >140 AU in the arthritic knee. In the ankles of the same animal, the ratio reached 600% between the healthy side and the arthritic side, with a dPGS-NIR signal value of 42 AU in the right joint compared to 300 AU in the left joint.

MSOT imaging of the oxygenated hemoglobin content, a good indicator of the blood circulation within

an animal, showed that the probe had extravasated and had almost completely disappeared from the blood flow in the ankles and knees at the time of imaging (Figures 1B, C, E, and F). Moreover, MSOT imaging showed that the volume of blood circulating in the vicinity of the inflamed joint was much higher than that in the healthy legs, as expected in conditions of acute inflammation. In the transverse image of the knee (Figure 1F), the saphenous vein and artery displayed ~2.6 mm^2 of lumen surface in the arthritic leg, as compared to 0.65 mm^2 in the healthy leg.

Overall, the arthritic animals with moderate inflammation displayed a mean ± SD difference in probe accumulation of ~48 ± 11%, with values in the left knee typically ranging between 110 AU and 132 AU, but values in the right knee being close to that in healthy animals (84 AU). In more extreme cases, the difference in probe accumulation reached almost 80%.

When 2-dimensional images were used to build a 3-dimensional volume, it became easier to visualize the extent and intensity of the inflammation in and around the joints. Using this technique, the basal level of dPGS-NIR could be seen in the healthy right leg of a mouse. In contrast, in the leg that received collagen induction, the increase in both the extent and intensity of the contrast agent signal could be observed all around the joints, as well as above the ankle (video available at http://www.cbi.ei.turn.de/index.php?id=109).

In parallel, MRI was performed on the same mice to achieve a sagittal view of the knee joint before and directly after injection of gadolinium contrast agent. In mice that developed RA, as determined by a combination of clinical manifestations and MRI results, we could typically detect synovitis in the knee of the left leg, close to where the induction compound was injected, whereas the healthy right knee (without collagen induction) lacked any findings associated with RA. Additionally, mild-to-severe soft tissue swelling of the area surrounding the joint, as well as edema near the joint, were noticeable through MRI in some of the arthritic mice, accompanied by redness, swelling, or lameness of the joint.

The severity of the clinical symptoms was associated with the degree of pathologic changes visible through MRI, thus enabling staging of the inflamed site. The specific animal presented in Figure 1 displayed a very extensive synovitis, highlighted after gadolinium injection on MRI (Figures 1G and H), with evident clinical symptoms. Swelling was also seen along the calf and tibia, and the lymphocyte:granulocyte ratio was 1.8,

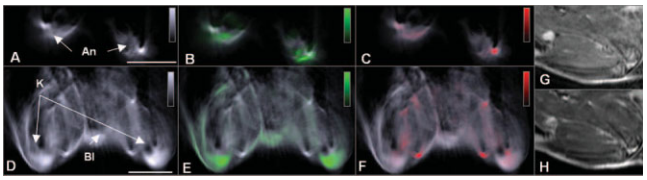

Figure 2. MSOT imaging of the ankles (**An**) and knees (**K**) of a representative healthy mouse, using NIR imaging with dPGS contrast agent. **A–F,** MSOT images of the left and right ankles (**A**) and knees (**D**) were acquired at an illumination wavelength of 860 nm for anatomic contrast. MSOT signals for dPGS-NIR accumulation and oxygenated hemoglobin in the ankles (**B** and **C**) and in the knees (**E** and **F**) are shown as fluorescence overlays on the anatomic images. Part of the bladder (**Bl**) is also visible. Bars = 5 mm. **G** and **H,** Sagittal T1-weighted magnetic resonance images were obtained from the left knee joint of the same mouse before (**G**) and after (**H**) gadolinium injection. **BV** = blood vessel.

confirming that a state of acute inflammation was present.

In contrast, in a healthy joint (without collagen injection or the limb on the right side of an injected animal), only a low, but distinguishable, signal was detected by MSOT in the knee and the ankle, which could be identified as dPGS-NIR by spectral unmixing (Figure 2). The amount of signal obtained from the articulations on each side was visually comparable, suggesting that there was only basal inflammation of L-selectins and P-selectins, thus implying that inflammation was not present and some signal could also be seen from the bladder, thus confirming the excretion route of the compound seen in preliminary fluorescence experiments (results available from the corresponding author upon request). In healthy animals, the absolute value of the difference between the dPGS-NIR signal intensity of the 2 sides was <30% in each animal, with a mean ± SD signal strength of ~84 ± 17 AU, similar to that obtained in the right side of the injected animals.

Furthermore, the amount of blood and volume of blood vessels in the joints from both sides of healthy mice were the same, confirming that inflammation was not present. The lumen of the visible saphenous blood vessels in the vicinity of the knee was comparable on both sides, at 0.65 mm^2 on the left side and 0.59 mm^2 on the right side, and these values were similar to those observed in the knees of healthy mice (Figure 2). On MR images obtained from healthy animals, neither synovitis nor swelling were visible (Figures 2G and H).

To assess the efficiency of the methods used in this animal cohort, we performed a systematic comparison of the stages of inflammation between the classic staging methods and the MSOT findings. The stages

were defined as absence of inflammation, low inflammation, or high inflammation (as illustrated in Figure 3). MSOT findings of healthy joints (i.e., those identified with the dPGS-NIR contrast agent as nonarthritic) corresponded to the absence of clinical symptoms and the absence of synovitis on MR images of the same joints. Animals identified as having low inflammation displayed limited clinical symptoms and mild-to-moderate synovitis on MR images. Animals whose MSOT images indicated high inflammation were found to have extended clinical symptoms and moderate-to-severe synovitis on MR images. Both sides of healthy animals were confirmed to have similar levels of dPGS-NIR accumulation, whereas in animals having low-to-moderate inflammation, the difference in dPGS-NIR accumulation between sides was nearly 50%, rising up to >70% in animals bearing high inflammation. Although the calculated standard deviation of this difference was significant (from 7% for low inflammation up to 15% for healthy animals), it remained low enough to be able to distinguish and categorize the animals in our panel.

Results of histopathologic analysis. Hematoxylin and eosin staining of the limbs of healthy mice and the right limbs of arthritic mice did not reveal any pathologic changes, whereas the left limbs of arthritic mice showed inflammatory infiltrates in the capsule. As displayed in Figures 4A–D, healthy joints showed normal morphologic structures, as demonstrated using hematoxylin and eosin staining, and very low and diffuse accumulation of the contrast agent in the knee joint. In contrast, the inflamed joints, as confirmed by hematoxylin and eosin staining, showed accumulation of the contrast agent to a large extent in the arthritic area, thus confirming the accumulation of the probe that was observed macroscopically in vivo on MSOT. These findings are indicative of an increased expression of L-selectins and P-selectins in the area. Moreover, the inflamed joints displayed the classic morphologic and physiologic features of arthritis. In particular, the volume of the synovial fluid appeared much higher, with a distortion of the capsule shape. Erosion of the cartilage to the bone could be seen, along with extensive infiltrates invading the capsule. Inflammatory cells, in particular leukocytes, were present and diffuse in the whole articulation.

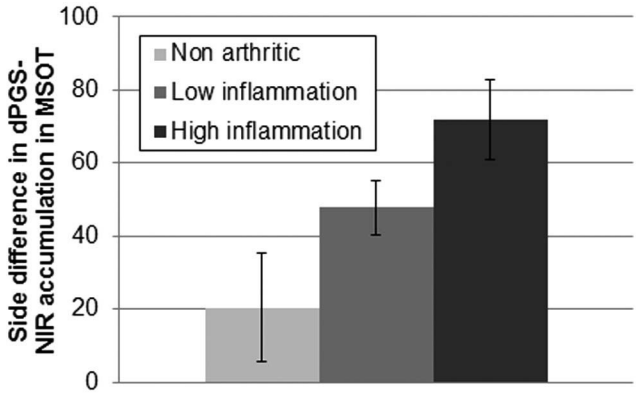

Figure 3. Difference in the MSOT dPGS-NIR signal between the healthy and inflamed sides in a series of animals in comparison with evaluations of inflammation by clinical examination and magnetic resonance imaging. The group of mice identified as having healthy (nonarthritic) joints on MSOT displayed no visible signs of inflammation and a normal blood cell count. The group of mice with low inflammation had less severe synovitis and a modified blood cell count. The group of mice with high inflammation displayed greater severity of synovitis and a low lymphocyte:granulocyte ratio. Bars show the mean ± SD percentage, representing the absolute values of the difference in dPGS-NIR accumulation between the limbs. See Figure 1 for definitions.

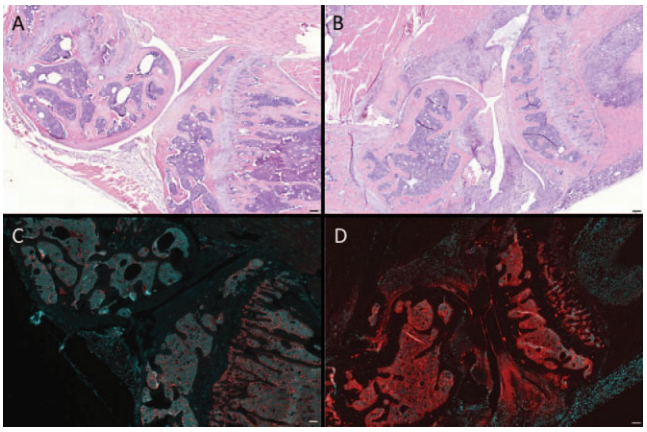

Figure 4. Microscopy analysis of the mouse knee joints. The knee joints of a healthy mouse (**A** and **C**) and a mouse with collagen-induced arthritis (**B** and **D**) were stained with hematoxylin and eosin for histopathologic analysis (**A** and **B**) and evaluated by fluorescence imaging using DAPI (blue channel) and polyanionic dendritic polyglycerol sulfate with a fluorescent indocarbocyanine conjugate as contrast agent (red channel) (**C** and **D**). Bars = 100 μm.

DISCUSSION

In this study using an inflammation-targeting fluorophore with validation in a murine model of RA, we investigated the advantages of MSOT over conventional imaging techniques for accurate spatial diagnosis of RA. The images clearly showed that accumulation of dPGS-NIR over time in the inflamed region of the limb depends on the stage of RA in the animal, and inducing

arthritis in only one side allowed for easy control and validation of each step of the experiment.

The different clinical manifestations of the disease, namely swelling, redness, and stiffness of the limb, translated into 2 types of signal increase observable on MSOT. First, animals with stiffness but limited swelling showed an increase in the optoacoustic signal strength of dPGS-NIR. Second, several animals presented swelling as a major sign of RA, more than stiffness or redness. In this case, the signal intensity itself was not drastically increased. However, and due to the extravasation of the probe and selectin-binding, the number of pixels containing significant dPGS-NIR optoacoustic signal was increased. In more extreme cases, such as the one presented in Figure 1, both the number of pixels displaying dPGS-NIR signal and its intensity were increased.

To go beyond the very user-dependent approach of estimating by eye the difference in signal between a normal limb and an inflamed limb, which is an important difficulty in, for example, ultrasound assessments, we decided to develop an automated process that would reduce the interoperator variability. By establishing a threshold for the noise level of a typical optoacoustic measurement, the shape of the region of interest defined by the user has only a very limited impact on the outcome of the measurement. Moreover, summing the values of the dPGS-NIR signal within the region of interest allowed our process to take into account both the number of pixels ("swelling" related) and the intensity of the pixels ("inflammation" related). This resulted in a resilient method that could be used to quantify the amount of dPGS-NIR accumulated in the joints.

Furthermore, by calculating the ratio of probe accumulation between the healthy side and the arthritic side, the MSOT protocol provided a staging capacity akin to the one currently used for MRI. When tested against MRI and clinical observation, we observed a high correlation between the optoacoustic staging process and the MRI findings and clinical observations, without the downfall of expensive MRI equipment or limited functional imaging capabilities. Because the imaged sections of interest are fairly close to the skin surface, the problem of light fluence is mitigated, as light does not have to travel more than ~5 mm, which is still beyond what is reachable using epifluorescence.

Scattering of ultrasound waves by the bones might have a limited impact (29), but since the excitation was attributable to only light, and not sound, only ultrasound waves generated by photoabsorbers may be reflected by the bones. This might induce a small blurring of the image due to a change in perceived localization of the emission source, but should remain orders of magnitude smaller than the signal originating directly from the contrast agent, given the frequencies used and the size and construction of the joint.

Even though optoacoustic imaging has been previously proposed for imaging of RA joints, the model chosen has only been used in the monitoring of angiogenesis in affected rat ankle joints (23). Although this was a valid approach that provided interesting results, it only allowed monitoring of a transverse slice of blood-related parameters. By moving to a murine model, we could monitor simultaneously the entire region of the ankles to the knees multispectrally in a very reasonable timeframe, which allowed us in turn to visualize inflammation through the use of a targeted contrast agent. This allowed staging of the disease in a user-independent manner, with very good correlation to the findings on MRI and clinical examination, which are methods that are currently being used to monitor treatment in patients with RA.

Although injection of contrast agents should usually be avoided in large population screenings, for obvious reasons (notably, costs, safety, and convenience), select screening in predisposed populations, as well as diagnostic and treatment monitoring in the best conditions possible, are warranted. For these reasons, use of a contrast agent can be justified, if the results indicate that there has been a clear improvement over previously used methods that do not involve labeling, such as MRI. In addition, with minimal adaptation of the equipment, we believe a similar optoacoustic imaging approach can be used to diagnose and monitor treatment in humans, providing a reliable and accessible technology in the clinic.

AUTHOR CONTRIBUTIONS

All authors were involved in drafting the article or revising it critically for important intellectual content, and all authors approved the final version to be published. Dr. Beziere had full access to all of the data in the study and takes responsibility for the integrity of the data and the accuracy of the data analysis.

Study conception and design. Beziere, von Schacky, Kosanke, Licha, Rummeny, Ntziachristos, Meier.

Acquisition of data. Beziere, von Schacky, Kosanke, Kimm, Nunes, Licha, Aichler, Walch.

Analysis and interpretation of data. Beziere, von Schacky, Kosanke, Kimm, Nunes, Aichler, Walch, Meier.

ADDITIONAL DISCLOSURE

Author Licha is an employee of Mivenion GmbH.

REFERENCES

1. Emery P, Quinn MA. Window of opportunity in early rheumatoid arthritis: possibility of altering the disease process with early intervention. Clin Exp Rheumatol 2003;21:S154–7.
2. Backhaus M, Kamradt T, Sandrock D, Loreck D, Fritz J, Wolf KJ, et al. Arthritis of the finger joints: a comprehensive approach comparing conventional radiography, scintigraphy, ultrasound, and contrast-enhanced magnetic resonance imaging. Arthritis Rheum 1999;42:1232–45.
3. Tan YK, Ostergaard M, Conaghan PG. Imaging tools in rheumatoid arthritis: ultrasound vs magnetic resonance imaging. Rheumatology (Oxford) 2012;51 Suppl 7:vii36–42.
4. Conaghan PG, Ejbjerg B, Lassere M, Bird P, Peterfy C, Emery P, et al. A multicenter reliability study of extremity-magnetic resonance imaging in the longitudinal evaluation of rheumatoid arthritis. J Rheumatol 2007;34:857–8.
5. Hammer HB, Terslev L. Role of ultrasound in managing rheumatoid arthritis. Curr Rheumatol Rep 2012;14:438–44.
6. Meier R, Thurmel K, Moog P, Noel PB, Ahari C, Sievert M, et al. Detection of synovitis in the hands of patients with rheumatologic disorders: diagnostic performance of optical imaging in comparison with magnetic resonance imaging. Arthritis Rheum 2012;64: 2489–98.
7. Fischer T, Ebert B, Voigt J, Macdonald R, Schneider U, Thomas A, et al. Detection of rheumatoid arthritis using non-specific contrast enhanced fluorescence imaging. Acad Radiol 2010;17: 375–81.
8. Meier R, Krug C, Golovko D, Boddington S, Piontek G, Rudelius M, et al. Indocyanine green–enhanced imaging of antigen-induced arthritis with an integrated optical imaging/radiography system. Arthritis Rheum 2010;62:2322–7.
9. Meier R, Thuermel K, Noel PB, Moog P, Sievert M, Ahari C, et al. Synovitis in patients with early inflammatory arthritis monitored with quantitative analysis of dynamic contrast-enhanced optical imaging and MR imaging. Radiology 2014;270:176–85.
10. Chen WT, Mahmood U, Weissleder R, Tung CH. Arthritis imaging using a near-infrared fluorescence folate-targeted probe. Arthritis Res Ther 2005;7:R310–7.
11. Ibarra JM, Jimenez F, Martinez HG, Clark K, Ahuja SS. MMP-activated fluorescence imaging detects early joint inflammation in collagen-antibody-induced arthritis in CC-chemokine receptor-2-null mice, in-vivo. Int J Inflam 2011;2011:691587.
12. Dernedde J, Rausch A, Weinhart M, Enders S, Tauber R, Licha K, et al. Dendritic polyglycerol sulfates as multivalent inhibitors of inflammation. Proc Natl Acad Sci U S A 2010;107:19679–84.
13. Licha K, Welker P, Weinhart M, Wegner N, Kern S, Reichert S, et al. Fluorescence imaging with multifunctional polyglycerol sulfates: novel polymeric near-IR probes targeting inflammation. Bioconjug Chem 2011;22:2453–60.
14. Ntziachristos V. Going deeper than microscopy: the optical imaging frontier in biology. Nat Methods 2010;7:603–14.
15. Razansky D, Buehler A, Ntziachristos V. Volumetric real-time multispectral optoacoustic tomography of biomarkers. Nat Protoc 2011;6:1121–9.
16. Ntziachristos V, Razansky D. Molecular imaging by means of multispectral optoacoustic tomography (MSOT). Chem Rev 2010; 110:2783–94.
17. Ma R, Taruttis A, Ntziachristos V, Razansky D. Multispectral optoacoustic tomography (MSOT) scanner for whole-body small animal imaging. Opt Express 2009;17:21414–26.
18. Wang X, Xie X, Ku G, Wang LV, Stoica G. Noninvasive imaging of hemoglobin concentration and oxygenation in the rat brain using high-resolution photoacoustic tomography. J Biomed Opt 2006;11:024015.
19. Buehler A, Herzog E, Razansky D, Ntziachristos V. Video rate optoacoustic tomography of mouse kidney perfusion. Opt Lett 2010;35:2475–7.
20. Herzog E, Taruttis A, Beziere N, Lutich AA, Razansky D, Ntziachristos V. Optical imaging of cancer heterogeneity with multispectral optoacoustic tomography. Radiology 2012;263: 461–8.
21. Taruttis A, Wildgruber M, Kosanke K, Beziere N, Licha K, Haag R, et al. Multispectral optoacoustic tomography of myocardial infarction. Photoacoustics 2013;1:3–8.
22. Rajian JR, Girish G, Wang X. Photoacoustic tomography to identify inflammatory arthritis. J Biomed Opt 2012;17:96013.
23. Rajian JR, Shao X, Chamberland DL, Wang X. Characterization and treatment monitoring of inflammatory arthritis by photoacoustic imaging: a study on adjuvant-induced arthritis rat model. Biomed Opt Express 2013;4:900–8.
24. Fournelle M, Bost W, Tarner IH, Lehmberg T, Weiss E, Lemor R, et al. Antitumor necrosis factor-alpha antibody-coupled gold nanorods as nanoprobes for molecular optoacoustic imaging in arthritis. Nanomedicine 2012;8:346–54.
25. Brand DD, Latham KA, Rosloniec EF. Collagen-induced arthritis. Nat Protoc 2007;2:1269–75.
26. Kamala T. Hock immunization: a humane alternative to mouse footpad injections. J Immunol Methods 2007;328:204–14.
27. Buehler A, Rosenthal A, Jetzfellner T, Dima A, Razansky D, Ntziachristos V. Model-based optoacoustic inversions with incomplete projection data. Med Phys 2011;38:1694–704.
28. Rosenthal A, Razansky D, Ntziachristos V. Fast semi-analytical model-based acoustic inversion for quantitative optoacoustic tomography. IEEE Trans Med Imaging 2010;29:1275–85.
29. Dean-Ben XL, Ma R, Razansky D, Ntziachristos V. Statistical approach for optoacoustic image reconstruction in the presence of strong acoustic heterogeneities. IEEE Trans Med Imaging 2011; 30:401–8.